Sub-pixel analysis to enhance the accuracy of evapotranspiration determined using MODIS images

Abdalhaleem A. Hassaballa[1]*, Abdul-Nasir Matori[2], Khalid A. Al-Gaadi[1,3], Elkamil H. Tola[1], Rangaswamy Madugundu[1]

(1. *Precision Agriculture Research Chair (PARC), King Saud University, Riyadh 11451, Saudi Arabia*;
2. *Geoinformatics Cluster, Department of Civil Engineering, Universiti Tecknologi PETRONAS, Tronoh 31750, Malaysia*;
3. *Department of Agricultural Engineering, College of Food and Agriculture Sciences, King Saud University, Riyadh 11451, Saudi Arabia*)

Abstract: A study was carried out to estimate the actual evapotranspiration (ET) over a 1074 km^2 of the humid area of Perak State (Malaysia), where water and evaporation cycle deeply influences the climate, natural resources and human living aspects. Images from both Terra and Aqua platforms of the Moderate Resolution Imaging Spectroradiometer (MODIS) sensor were used for ET estimation by employing the Surface Energy Balance Algorithm for Land (SEBAL) model. As a part of the accuracy assessment process, in-situ measurements on soil temperature and reference ET (ET_0) were recorded at the time of satellite overpass. In order to enhance the accuracy of the generated ET maps, MODIS images were subjected to sub-pixel analysis by assigning weights for different land surface cover (urban, agriculture and multi-surface areas) reflections. The weighting process was achieved by integrating ET from pure pixels with the respective site-specific ET_0 of each land cover. The enhanced SEBAL model estimated ET exhibited a good correlation with the in-situ measured Penman-Montieth ET_0, with R^2 values for the Aqua and the Terra platforms of 0.67 and 0.73, respectively. However, the correlation of the non-enhanced ET maps resulted in R^2 values of 0.61 and 0.68 for the Aqua and the Terra platforms, respectively. Hence, the results of this study revealed the feasibility of employing the sub-pixel analysis method for an accurate estimation of ET over large areas.

Keywords: evapotranspiration, sub-pixel analysis, MODIS image, MODIS sensor, remote sensing, land surface cover
DOI: 10.3965/j.ijabe.20171002.2890

Citation: Hassaballa A A, Matori A, Al-Gaadi K A, Tola E H, Madugundu R. Sub-pixel analysis to enhance the accuracy of evapotranspiration determined using MODIS images. Int J Agric & Biol Eng, 2017; 10(2): 103–113.

1 Introduction

Evaporation and transpiration are two processes that concurrently take place and cannot be differentiated. The amount of evaporation from croplands is principally based on the solar radiation fraction that hits the soil surface. This fraction is decreasing as the crop evolves and grows, where the crop canopy increasingly shades the ground surface beneath the plant. Water is mainly lost through soil evaporation at germination and early stages of plant growth. When the crop is well toned and totally covers the soil surface, the transpiration, which acts at the plants' leaves and stomata, becomes the dominant water losses process from croplands[1].

Investigating ET at regional scale becomes an important matter as it helps in understanding the global changes in the environment as well as when planning to develop water supplies for agricultural schemes or/and other related activities. In addition, ET analysis is always required to develop a hydrological model at any scale for a specific region[2-7].

Received date: 2016-10-02 **Accepted date:** 2017-02-14
Biographies: Abdul-Nasir Matori, PhD, Associate Professor, research interests: geomatics, Email: nasrat@petronas.com.my; **Khalid Ali Al-Gaadi**, PhD, Professor, research interests: precision agriculture, Email: kidaag@gmail.com; **Elkamil Hamed Tola**, PhD, Associate Professor, research interests: precision agriculture, Email: elkamiltola@gmail.com; **Rangaswamy Madugundu**, PhD, Assistant Professor, research interests: precision agriculture, Email: ranga.nrsa@gmail.com

***Corresponding author: Abdalhaleem Abdalla Hassaballa**, PhD, Assistant Professor, research interests: precision agriculture. Mailing address: P.O.Box 2460, Riyadh 11451, Saudi Arabia. Tel: +966-114691943/542053994(M), Email: ahassaballa@ksu.edu.sa.

Since the fundamental of satellite remote sensing is based on knowledge of the spectral response of surface entities, reflectance form vegetation cover and surface temperature (T_s) are considered as the most important two parameters obtained from the optical and the thermal spectral portions of the spectrum, respectively. However, no intensive work has been devoted to study the relationship between vegetation and T_s with respect to land use/cover. This is because these two parameters are tightly correlated to both the moisture availability and the vegetation condition. Price[8] pointed out that there would be no advantage of using sophisticated simulation model for the estimation of ET, if the required surface parameters are not available for the region.

Studies of remote sensing in estimating ET usually include four basic common methods. The first one is known as the simplified energy balance method, which is the basic formula initially extracted at field scale by Jackson[9], and later employed successfully by Pinker[10] for mapping daily ET over large areas via surface temperature measurements. This method was also found to be very successful in estimating crop water use in irrigated areas[11]. However, the estimation of energy balance components from the remotely sensed data requires series of computations and site-specific meteorological data such as reference ET (ET_0), vapor pressure deficit, wind speed, relative humidity, net radiation, etc.[12] The second one is the empirical method, which is an empirical relationship between the spectral variables measured from satellites and the ET. As examples, Idso[13] developed a linear relationship between evaporation and the net thermal radiation. In another study, Menenti[14] determined ET as a linear function of the remote sensing estimated T_s and the surface albedo. Seguin and Itier[15] demonstrated that, at a specific location, there is a strong relationship between the midday T_S and the daily ET. Also, Kerr[16] identified a detailed relationship between the Normalized difference vegetation index (NDVI) extracted from the NOAA High Resolution Picture Transmission (HRPT) data and the actual ET. Although the empirical methods are widely and successfully applied for ET estimation, most of them are site-specific and can't be used for areas with different climatic conditions. The third one is the deterministic method, which usually depends on more complicated models such as Soil-Vegetation-Atmosphere Transfer models (SVAT). This model has been designed to simulate the interaction between plant canopy processes and the environment, and to calculate different elements of energy budget[17]. The fourth method is the energy balance equation, which is used for ET estimation (equivalent to the latent heat flux LE) using various surface properties such as albedo, leaf area index, vegetation indices and T_S[18].

The most issue hindering the measurement of ET at ground stations is its dependency on some surface parameters that are so difficult to measure over large and heterogeneous areas[2,19-22]. Thus, the effectiveness of such methods will not exceed the areas where parameters are measured. In addition, the ground-based estimation of ET is considered as a vegetation-type-specific, and the estimation accuracy is affected by surface resistance, which introduces more difficulties in applying the ground-based ET on a regional scale.

On the other hand, the estimation of ET from the multi-temporal resolution sensors such as MODIS (Moderate Resolution Imaging Spectroradiometer) and NOAA (National Oceanic & Atmospheric Administration) does not represent the real signature of surface features, because of the coarse spatial resolution. As a result, the value of ET is always produced from a holistic land surface cover within the image pixel, what leads to over/under estimations of ET.

This study aimed particularly at providing an enhanced and cost-effective qualitative estimation of ET through the sub-pixel analysis. The study employed the weighting approach on ET maps of three different land covers generated through the Surface Energy Balance Algorithm for Land (SEBAL). The three land cover classes included cultivated area (agriculture) represented by Seberang Perak's paddy field (SP), urban area represented by Sitiawan (SITI) city and multi-cover area represented by a weather station allocated at the field of Universiti Teknologi PETRONAS (UTP). The study also intended to enhance the value of the MODIS satellite extracted T_S through a correlation process against the soil

temperature measured in-situ at the time of satellite overpass.

2 Materials and methods

2.1 Study area

The study area covered two distinctive districts of Perak state (Malaysia), which were Perak Tengah and Manjung. The two neighbor districts lie between latitudes 4º00'-4º30'N and longitudes 100º30'-101º00'E (Figure 1) and separated by Sungai Perak (Perak River) which ran along the study area from the north to the south and surrounded Manjung district from the southern side to the coast downstream.

Perak Tengah district encompassed an area of 1282.05 km^2 comprised 11 localities. This district was located in the center of the state of Perak, in an elongated shape from north to south, where the Sungai Perak River spited it into two halves on the left and right. Manjung was surrounded by only two districts Kerian from the north and Perak Tengah from the east, while the coastline occupied the remaining directions. The total area under the study was about 1074 km^2[23].

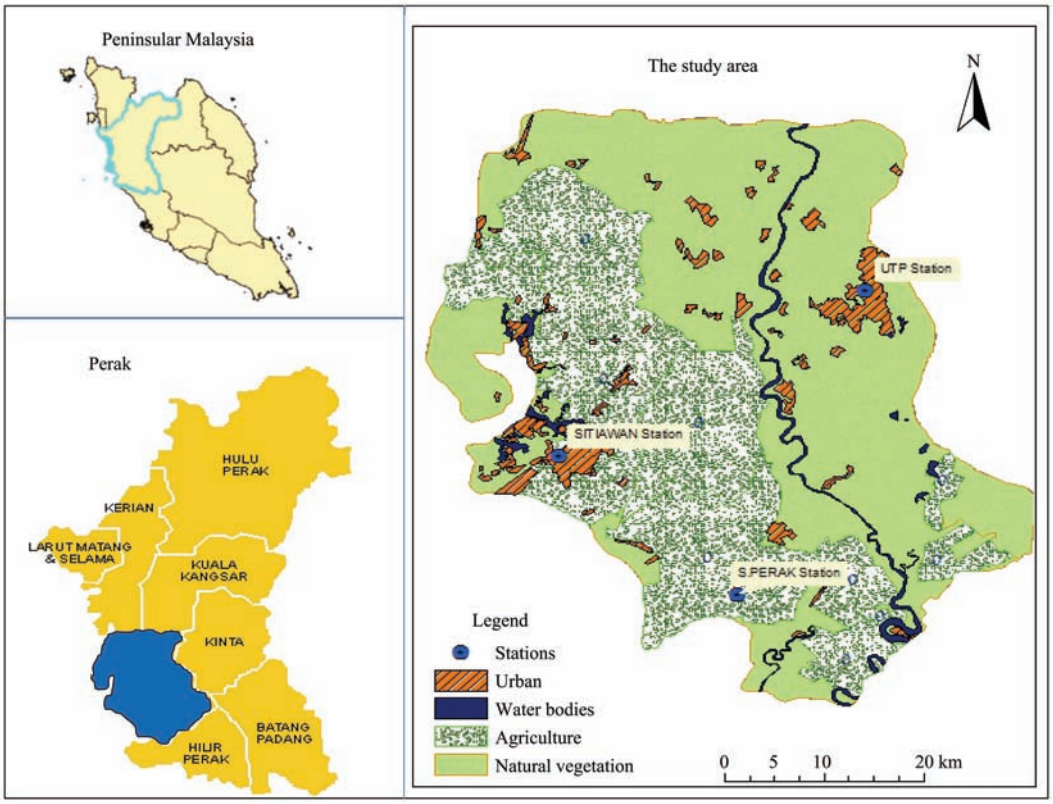

Figure 1 The study area with classified land use land cover map for surface representation

2.2 Topography, climate & Land use/land cover

The study area was occupied mainly by four types of land use/cover which were the urban areas represented by some cities and rural areas scattered along the river (Sungai Perak). Some villages lie inside agricultural lands and forest areas.

Other part of the area was sort of bare soils scattered beside the residential areas and some hilly areas. The vegetation cover took the bigger portion of the area and was divided into two types: The first portion was the natural vegetation cover, which included the jungles, natural trees, grassland and some pasture lands. The second portion of the vegetation cover was agricultural fields of paddy, oil palm and coconut managed by some agricultural companies. The last type of the land surface cover was the water bodies, which was represented mainly by Perak River beside a random distribution of some lakes over the area as abandoned Tin mines.

The weather at the study area was warm and sunny, although at night was cool the entire year through, with periodic rains in the evenings. Temperature was relatively constant, which varied from 23°C to 33°C, with humidity typically greater than 80%. Annual rainfall mostly measured at about 3200 mm[24]. The periodic wind flow patterns along with the local topographic characteristics determined the rainfall distribution patterns

across the country.

2.3 MODIS satellite images

MODIS (Level 1B) images were acquired from the Level-1 and Atmosphere Archive and Distribution System website (LAADS; http://ladsweb.nascom.nasa.gov) for the estimation of ET. The MODIS (Level 1B) products included daily composites of land surface temperature (T_S; Bands 31 and 32) of MOD11A1 and MYD11A1 products (1 km resolution). In addition, surface reflectance products (MOD09 and MYD09) comprised red (RED), near infrared (NIR), and blue (B) bands (500 m resolution). The quantity and period of acquired MODIS products are listed in Table 1.

Table 1 Web-based MODIS images downloaded for the study area

Sensor	Quantity	Period of acquisition	Processing level	Type
MODIS Terra/Aqua	22	1st June – 30th August 2012	(Level 1B)	Daily
	14	1st February – 30th April 2011		

2.4 Ancillary data collection

For calculating ET_0, maximum and minimum daily air Temperature data (February-April 2011 and June-September 2012), mean daily wind speed and mean daily relative humidity, for Sitiawan and Seberang Perak station, were collected from the Malaysian Meteorological Department (MMD)[23]. UTP station in turn, provided a temperature gauge for measuring temperature, an anemometer for measuring wind speed, a hygrometer for measuring humidity, a barometer for measuring atmospheric pressure, a rain gauge for measuring liquid-equivalent precipitation and a pyranometer for measuring solar radiation, in addition to the facilities of measuring evaporation, soil temperature and soil moisture at a depth of 0.3 m. The weather parameters, required for the calculation of ET_0, were collected for the entire study period.

2.5 In-situ measurements

Soil temperature was measured close to the meteorological stations at three variable depths in the soil (5 cm), which was assumed to represent surface temperature, 10 cm represented the near surface and 15 cm which was achieved at agricultural fields only. The objective behind measuring soil temperature was to produce an enhanced satellite T_S through applying in-situ measurements of soil temperature at the same time of the satellites overpass on the study area. This kind of application was made to simulate the absolute atmospheric correction. In which, the path radiance was corrected using calibration target, where, regression was used to predict the correct value of the image[25,26]. Moreover, the application also meant to correlate the measured T_S within three different depths on the soil to examine the workability of the split window technique in the retrieval of T_S, thus, more accurate T_S value can be used for ET extraction.

2.6 Formulae for ET extraction

MODIS Land surface temperature (T_S), which is a product of Aqua MODIS (e.g. MYD11A1 products) and Terra-MODIS (e.g. MOD11A1 products), is offered per-pixel temperature values every day. In order to predict the T_S and Emissivity (ε_s) from the acquired images, a mean value of 5×5 pixels corresponding to the location of weather station was extracted and considered as pure pixel. The simulation and execution of algorithms were performed on the pure-pixel and correlated with the ground measured ET_0 during the accuracy assessment. In addition, in-situ measurements on soil temperature also collected on times of satellite overpass using a mini thermometer with a measurement rang of –50ºC to +250ºC and an accuracy of ±1.0ºC.

2.7 Split-window algorithm for deriving MODIS T_S

The general form of the split-window equation can be written as shown in Equation (1)[27]:

$$T_S = T_{31} + A(T_{31} - T_{32}) + B \quad (1)$$

where, T_S is the land surface temperature, K; T_{31} and T_{32} are the brightness temperature from channel 31 and 32 respectively, K; A and B are the coefficients determined by the impact of atmospheric conditions responsible for the thermal radiance transmission in channels 31 and 32.

2.8 Normalized difference vegetation index (NDVI)

The NDVI layer was generated from the spectral reflectance of the red (0.62-0.67 μm) and near-infrared, NIR (0.841-0.876 μm) regions of the spectrum, as it is shown in Equation (2)[28].

$$\mathrm{NDVI} = \frac{(\mathrm{NIR} - \mathrm{RED})}{(\mathrm{NIR} + \mathrm{RED})} \quad (2)$$

2.9 Temperature enhancement

Satellite T_S was used in conjunction with soil temperature recoded at three depths (5 cm, 10 cm, and 15 cm) measured in-situ. A linear regression sketch between T_S and the soil temperature was used, in order to apply the absolute atmospheric correction for the path radiance removal. This procedure was confirmed and suggested by Jensen[25] as a method for T_S calibration in optical sensors. Since satellite-based T_S gives a mixed signature and reflects a combined temperature of soil and vegetation, such kind of ground truthing which contains measurements of soil temperature was used to surpass the vegetation's signal attenuation of emissivity. Thus, a linear regression between satellite-based T_S and ground measurements of soil temperature was conducted to enhance the resultant surface temperature where the temperature from satellites were extracted and unified by the bulk averaging method to enable a good comparison with the point nature of ground T_S measurements. Figure 2 shows an example of the resultant correlation between the three T_S sets for UTP location. The values of soil temperature at the three soil depths were correlated against the corresponding T_S value extracted from satellite image (T_S as a single value after bulk averaging). The satellite extracted T_S was found to be highly resemble to the measured soil temperature at 5 cm depth, which was thus used along with the NDVI to estimate ET.

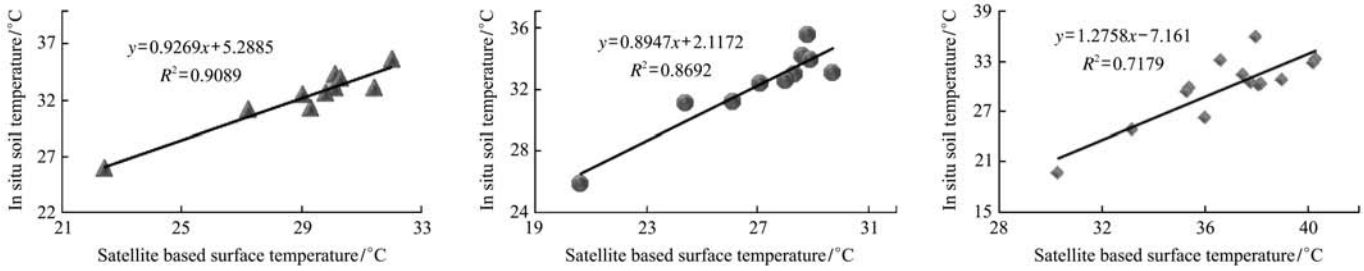

a. At 5 cm soil depth b. At 10 cm soil depth c. At 15 cm soil depth

Figure 2 Correlation between in-situ soil temperature and satellite *Ts* for accuracy enhancement along the three depths of MODIS over UTP location

2.10 Estimation of ET using SEBAL

ET estimation (equivalent to the latent heat flux LE) by remote sensing is dependent on evaluating various surface properties of the energy balance equation such as albedo, leaf area index, vegetation cover, and T_S. When thinking about instantaneous conditions, the energy balance formula is written as shown in Equation (3)[29]:

$$\lambda ET = R_n - G - H \quad (3)$$

where, λET is the latent heat flux calculated as a residual of the energy budget, W/m^2; R_n is the net radiation, W/m^2; G is the soil heat flux, W/m^2; H is the sensible heat flux to the air, W/m^2.

The net radiation is estimated spatially as the difference between the incoming shortwave radiation (*Rs*) and the outgoing long wave radiation (*Rl*, in the form of air transmissivity (ε_a) and temperature (T_a)) as expressed in Equation (4):

$$R_n = (1-\alpha)R_{S\downarrow} + \varepsilon_a \sigma T_a^4 - \varepsilon_S \sigma T_S^4 \ (\mathrm{W \cdot m^{-2}}) \quad (4)$$

where, R_S represents the solar or shortwave radiation, MJ/m^2·d; α is the albedo or canopy reflection coefficient, which is 0.23 for the hypothetical grass reference crop [dimensionless]; T_a is the air temperature, K; T_S is the surface temperature, K; ε_S is the surface emissivity calculated as the logarithmic value of NDVI from the relation ε_S=1.0094+0.047×*Ln*(*NDVI*)[28]; σ is the Stefan–Boltzman constant (5.67×10^{-8} W/m^2·K^4) and ε_a is the air transmissivity taken as in [30].

G is the soil heat flux (W/m^2), and was calculated from the relation given in Equation (5)[31]:

$$G = R_n \left[\frac{T_S}{\propto}\right](0.0038 \propto +0.0074 \propto^2)(1-0.98\mathrm{NDVI}^4) \quad (5)$$

H is the sensible heat flux (W/m^2), which was calculated from the relation presented in Equation (6)[32]:

$$H = \frac{\rho c_p \mathrm{d}T}{r_{ah}} \quad (6)$$

where, ρ is the air density, kg/m^3; c_p is the specific heat of air, 29.3 J/kg·°C; dT is the near surface temperature difference, K; r_{ah} is the aerodynamic resistance to heat

transport, s/m.

2.11 Assessment of daily ET from satellites

The obtained latent heat flux (λET) for the time of satellite overpass (W/m^2) as a residual of energy budget algorithm was converted to hourly instantaneous value of the evapotranspiration (ET_{inst}) as given in Equation (7)[33]:

$$ET_{inst} = 3600\frac{\lambda ET}{\lambda} \quad (7)$$

where, ET_{inst} is the instantaneous ET, mm/h; 3600 is a time conversion from seconds to hours; λ is the latent heat of vaporization or the absorbed heat when a kilogram of water evaporates, J/kg.

Finally, the daily ET_d was estimated in the form of temporal integration of the resultant instantaneous ET (ET_{inst}), as proposed by Sobrino[34], and was used to estimate the daily ET using satellite potentials in collaboration with the terrestrial data (Equation (8)). This integration was based on the assumption that the evaporative fraction at the daily scale is mostly resemble to the one that derived instantaneously at the time of satellite's data acquisition[35,36].

$$ET_d = \int_0^{24} ET_{inst}(t)\mathrm{d}t \quad (8)$$

where, ET_{inst} (t) was used in hourly time base and ET_d is the daily ET_0.

The evaporative fraction Λ was computed from the instantaneous surface energy balance at time of satellite overpass for each pixel (Equation 9)[37,38].

$$\Lambda = \frac{\lambda E}{R_n - G_o} = \frac{\lambda E}{\lambda E + H_o} \quad (9)$$

where, λE is the energy assigned for water evaporation. It is reliant on the atmospheric and soil moisture conditions balance.

2.12 Daily ET_0 from meteorological data

In order to verify and validate the ET extracted from satellite images, reference ET (ET_0) was computed utilizing three classical/well-known methods, Penman-Monteith (PM)[2], Hargreaves[39,40] and Turc[41]. Because Penman-Monteith (PM) approach has successfully combined the aerodynamic approach with the energy balance method to estimate ET_0, it is considered as a global standard for estimating ET_0 based on four meteorological data (temperature, wind speed, radiation and relative humidity)[42]. Thus, it was used as the reference for ET_0 estimates throughout the whole ET findings. Then, all meteorological parameters collected from the ground stations were applied in PM, Hargreaves and Turc methods with daily bases considering the satellite's overpassing time chronology. The PM[2], Hargreaves[39,40] and Turc[41] formulae are shown below in Equations (10)-(12), respectively.

$$ET_0 = \frac{0.408\Delta(R_n - G) + \gamma\frac{900}{T+273}u_2(e_s - e_a)}{\Delta + \gamma(1 + 0.34u_2)} \quad (10)$$

where, ET_0 is the reference evapotranspiration, mm/d; R_n is the net radiation at the crop surface, MJ/m^2·d; G is the Soil heat flux density, MJ/m^2·d; T is the mean daily air temperature at 2 m height, °C; u_2 is the wind speed at 2 m height, m/s; e_S is the saturation vapour pressure, kPa; e_a is the actual vapour pressure, kPa; ($e_S - e_a$) is the saturation vapour pressure deficit, kPa; Δ is the slope of the vapour pressure curve, kPa/°C; γ is the psychometric constant, kPa/°C.

$$ET = 0.0023\left(\frac{R_a}{\lambda}\right)(T + 17.8)(T_{max} - T_{min})^{0.5} \quad (11)$$

where, ET is the daily potential evapotranspiration rate, mm/d; R_a is the extraterrestrial radiation in the hour period, MJ/m^2·d; T is the mean temperature, ^{o}C; λ is the latent heat of vaporization, kJ/kg, T_{max} is the daily maximum temperature, ^{o}C; and T_{min} is the daily minimum temperature.

$$ET_p = \propto [(23.9001R_s) + 50]\left(\frac{T}{T+15}\right) \quad (12)$$

where, α is a constant, 0.01333; Rs is measured radiation, MJ/m^2 ·d.

2.13 Implementation strategy

The study intended to generate a suitable ET estimation algorithm for the study area concerning the influence of the T_S extracted from the thermal bands of satellite sensors. The T_S enhancement was made through an empirical equation obtained by linear correlation relationships among the T_S and soil temperature collected from ground measurements. The following flow chart (Figure 3) shows the steps achieved towards the generation and the validation of the analyzed sub-pixel ET from MODIS.

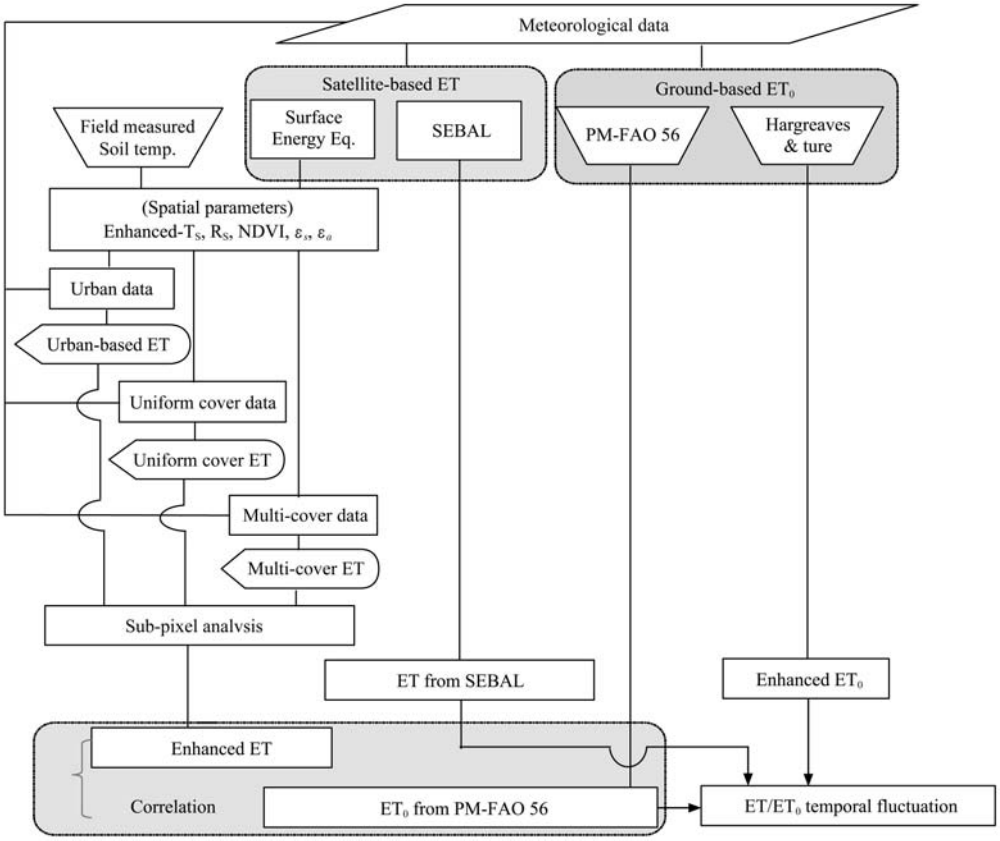

Figure 3 Flow chart of the energy budget equation application for assessing ET

2.14 Derivation of weighted ET map

The total ET map of the pixel-based image was finally calculated as a summation of the three ET values at the pixel base (ET_{SUM_i}). Then, the fraction (Fr_i) of each ET value shared the single pixel was calculated as a percentage of the pixel ET value of the particular station (UTP, Sitiawan and S. Perak) to the total ET at the pixel. Equations (13)-(20) describe mathematically the steps towards the calculation of ET fractions over the study area.

$$ET_{SUM_i} = \sum_{i=1}^{n} (ET_{UTP_i}, ET_{SITI_i}, ET_{SP_i}) \quad (13)$$

$$Fr_{UTP_i} = {ET_{UTP_i}}/{ET_{SUM_i}} \quad (14)$$

$$Fr_{SITI_i} = {ET_{SITI_i}}/{ET_{SUM_i}} \quad (15)$$

$$Fr_{SP_i} = {ET_{SP_i}}/{ET_{SUM_i}} \quad (16)$$

The weighting (Wi) of each land surface cover type at the pixel base was determined by applying the fraction of each station to the corresponding full ET pixel. Finally, the sub-pixel analyzed evapotranspiration (ETi) at the image pixel base was calculated as a summation of the three different weights of ET pixels.

$$W_{UTP_i} = Fr_{UTP_i} \times ET_{UTP_i} \quad (17)$$

$$W_{SITI_i} = Fr_{SITI_i} \times ET_{SITI_i} \quad (18)$$

$$W_{SP_i} = Fr_{SP_i} \times ET_{SP_i} \quad (19)$$

$$ET_i = W_{UTP_i} + W_{SITI_i} + W_{SP_i} \quad (20)$$

More clarification is shown in (Figure 4), in which ET was extracted according to the weights of the land surface cover types available within this pixel as a result of the sub-pixel analysis as in (a) in Figure 4. On the other hand, task (b) shows the same image pixel in its ordinary extraction process which produced ET value from the holistic features of the land surface cover.

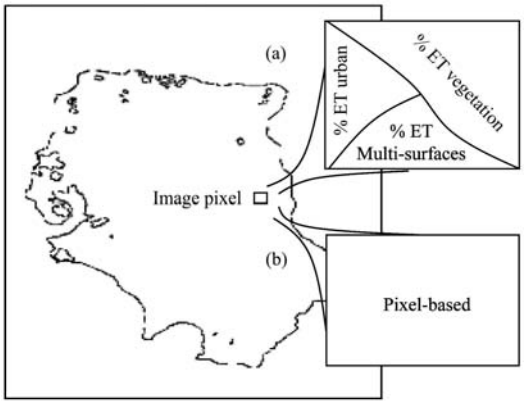

Figure 4 ET extraction based on (a) sub-pixel analysis and (b) the ordinary pixel-based ET

3 Results and discussion

3.1 Spatial ET versus ground ET_0

Comparative plots of the resultant satellite ET (enhanced pixel/generalized reflection pixel) from SEBAL model beside the ground-based values of ET_0 calculated using three ground estimators are shown in Figure 5. The SEBAL approach used to assess ET was produced from satellite based-T_S and satellite enhanced-T_S and analyzed sub-pixel. MODIS Terra images were captured at morning time (10:30 AM), where temperature and solar radiation values were relatively low. For the mid-day session, MODIS Aqua images which have an overpass time around (2:20 PM) were acquired and analyzed to extract ET and then plotted against the measured ET_0 from Penman-Monteith, Hargreaves and Turc methods.

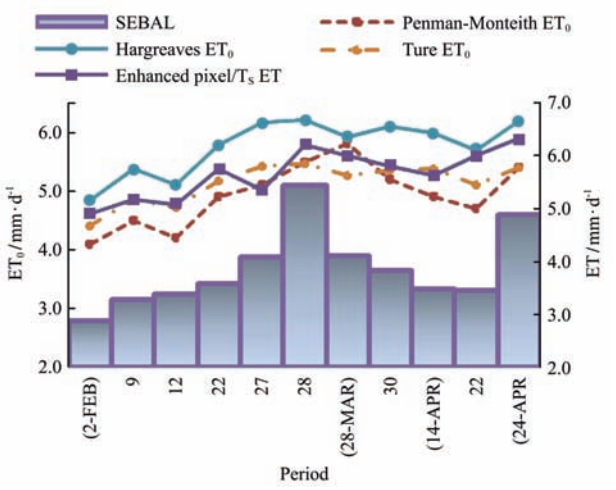

a

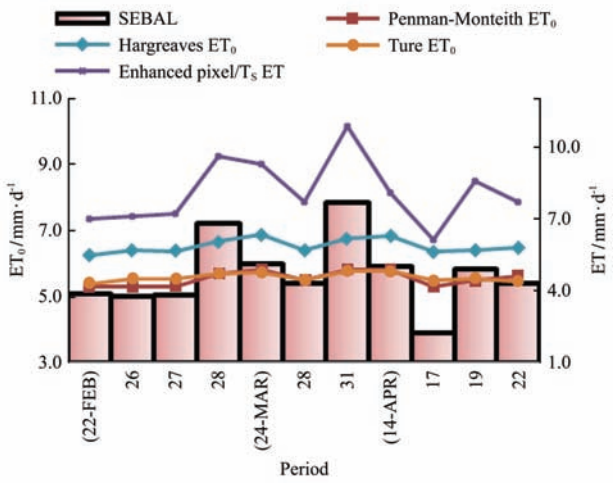

b

Figure 5 Scatterplots of satellite-estimated ET and ordinary-measured ET_0 at study locations from (a) MODIS Terra and (b) Aqua

Due to the tremendous interference between the different vegetation species and surface entities within the multi-surface and the urban portion of the study area, and because of the inconsistency of assigning crop coefficients to ET_0 of all these variable types of vegetation, the study intended to correlate the satellite ET with the reference ET_0. It could be seen in Figure 5 below, the alteration in satellite's ET values and attitudes are very noticeable with correspondence to the ordinary ones.

It can be noticed that, the extracted ET produced better results when the enhanced pixel/T_S was used along with the NDVI, this could be seen obviously from the validation of the resultant ET using the reserved satellite images with reference to the ET_0 from FAO Penman-Monteith method.

The extracted ET from the images was found to be resembled to the FAO-56 ET_0 to a very far extent, particularly from MODIS Terra images which overpasses the area at morning times with an average ET of 6 mm/day. On the other hand, an overestimation of the spatial ET values was observed over parts of the study area from MODIS Aqua images. This might be due to the high dose of T_S and solar radiation coming in the form of short waves and the high surface albedo captured by this sensor during the mid-day. Simple justification is that, the field-based measurements of ET_0 involved the incorporation of wind speed and relative humidity found to be very effective parameters that influence the evaporative fraction of land surface cover. On the other hand, the wind speed in the spatial assessment of ET was only considered for assessing the ground heat flux which was a small portion of the energy flux which is mostly neglected for daily ET.

The normal-pixel ET produced from SEBAL model showed relatively low values (underestimation compared to FAO ET_0) over locations where images from MODIS satellite were used (both Terra and Aqua). This might be attributed to the scale disparity between the thermal bands used for T_S estimation (1 km×1 km) and the optical bands used for NDVI extraction (250 m×250 m). For SEBAL model, the course resolution may have dominated the vegetation signature causing more

representation of the cold temperature (T_{cold}). Figure 6 shows examples of the resultant ET maps extracted from MODIS Terra and Aqua images.

The spatial distribution of ET revealed a great variation in ET values along the three different land surface covers, where the least ET values (the gray and blue colors of Figures 6a and 6b, respectively) were observed to be over the urban areas, while the agricultural land sector produced the highest ET, illustrated by the brown color for both (a) and (b).

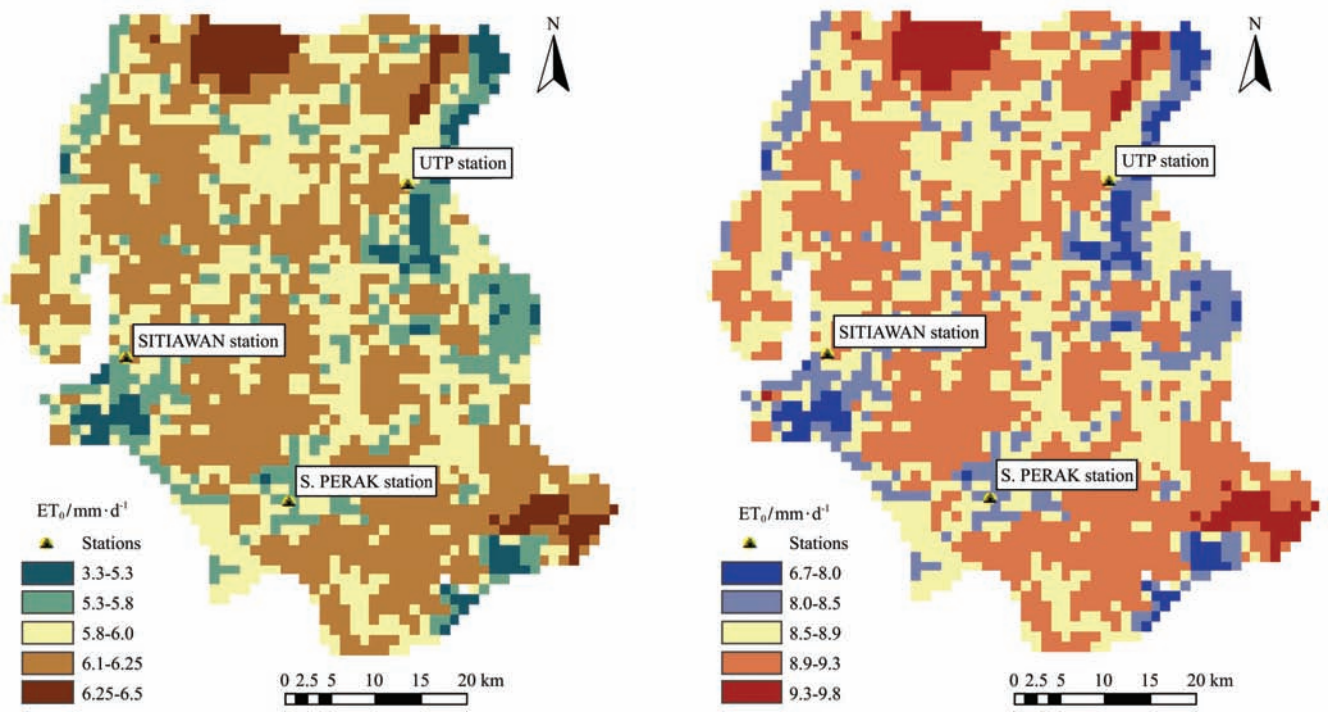

Figure 6 ET extracted from (a) Enhanced-pixel ET of MODIS Terra, and (b) Enhanced-pixel ET of MODIS Aqua

3.2 Algorithms validation

The study intended to examine the accuracy of the generated ET from the analyzed sub-pixel qualitatively through validating the ET values calculated using the weighting approach for all cells in the study area with the generalized-pixel ET. In which, the reserved datasets of MODIS Terra and field measurements of morning times were used. While, MODIS Aqua images were used for the mid-day session where temperature and radiation intensity are slightly high. Figure 7 shows the validation of MODIS Terra and Aqua satellites over the study area for ET estimations under the sub-pixel analysis and generalized pixel versus FAO 56 ET_0 as a reference value. All ET values, which were estimated from the sub-pixel analysis (weighting approach) produced better results when compared to the ordinary estimated ET with high R^2 values (67%-73%).

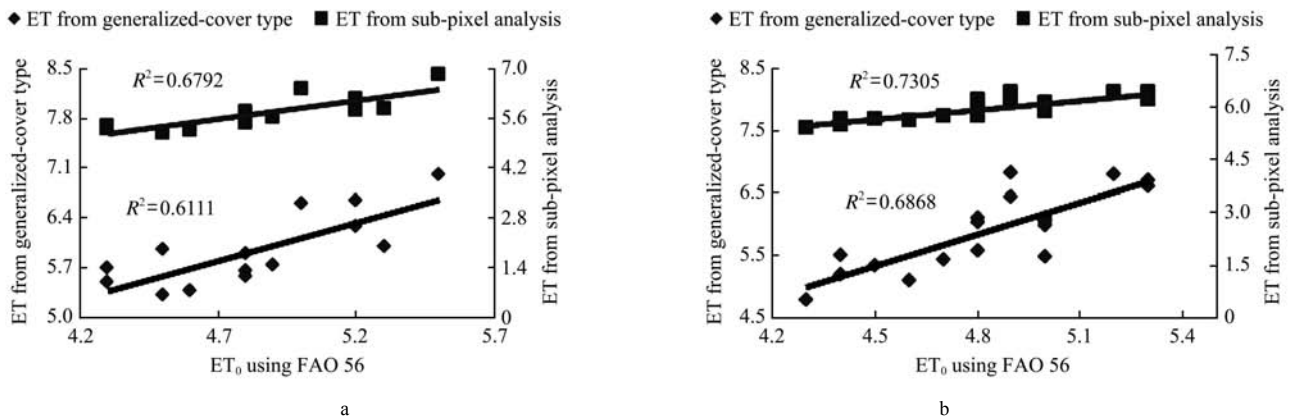

Figure 7 ET validation using generalized land surface cover and sub-pixel analysis from MODIS Agua (a) and MODIS Terra images (b)

The represented validation achieved by the two spatial ET types, assured the usefulness of the sub-pixel analysis (weighting approach) in producing a valuable estimation of the ET from the coarse image's pixel compounds; specially for producing values closer to the ET_0 measured at three ground stations with different meteorological aspects. It could be distinguished from the browsed accuracies that, the applied sub-pixel analysis is mostly in a good agreement with the concept of point-measurement of ET with regard to its spatial and temporal distribution along the variable surface cover lands.

4 Conclusions

A study was carried out to provide a satellite-based cost-effective method to estimate the actual evapotranspiration (ET) over a humid area using optical/thermal infrared images of MODIS sensors. The study employed the weighting approach in order to produce a type-specific land surface cover ET from three dissimilar surface cover types. The specific conclusions of the study are as follows:

1) The average ET from MODIS Terra was found to be 6 mm/d over the study area; however, MODIS Aqua images provided overestimated spatial ET values over parts of the study area. The overestimation ranged from 16% to 54%.

2) An experimental validation of satellite estimated ET and calculated ET_0 produced R^2 values of 0.73 for the sub-pixels analyzed ET and 0.68 for ET derived from generalized-cover pixel of MODIS Terra images. For MODIS Aqua data, the R^2 values were determined at 0.67 for the sub-pixels analyzed ET and 0.61 for ET obtained from generalized-cover pixel.

Acknowledgment

This project was financially supported by King Saud University, Vice Deanship of Research Chairs. The first author acknowledges the support given by Universiti Teknologi PETRONAS for providing research facilities for the study. The first author also gratefully acknowledges the assistance provided by the Malaysian Agency for Remote Sensing and the Malaysian Meteorological Department for providing all required spatial and meteorological data.

[References]

[1] Allen R G, Pereira L S, Raes D, Smith M. Crop evapotranspiration-Guidelines for computing crop water requirements. FAO Irrigation and Drainage Paper, No. 56. 1998. pp. 329.

[2] Penman H L. Natural evaporation from open water, bare soil and grass. Proceedings of the Royal Society of London, 2010; 193(1032): 120–145.

[3] Priestley C H B, Taylor R J. On the assessment of surface heat flux and evaporation using large-scale parameters. Monthly Weather Review, 1972; 100(2): 81–92.

[4] Monteith J L. Evaporation and surface temperature. Quarterly Journal of the Royal Meteorological Society, 1981; 107(451): 1–27.

[5] Famiglietti J S, Wood E F. Evapotranspiration and runoff from large land areas: Land surface hydrology for atmospheric general circulation models. Land Surface-Atmosphere Interactions for Climate Modeling, 1990; 179–204.

[6] Braun P B, Maurer B, Müller G, Gross P, Heinemann G, Simmer C. An integrated approach for the determination of regional evapotranspiration using mesoscale modelling, remote sensing and boundary layer measurements. Meteorology and Atmospheric Physics, 2001; 76(1): 83–105.

[7] Curran P, Foody G M. Environmental issues at regional to global scales. John Wiley & Sons Ltd, 1994; p.238.

[8] Price J C. Using spatial context in satellite data to infer regional scale evapotranspiration. IEEE Transactions on Geoscience and Remote Sensing, 1990; 28(5): 940–948.

[9] Jackson R D, Reginato R J, Idso S B. Wheat canopy temperature: a practical tool for evaluating water requirements. Water Resources Research, 1977; 13(3): 651–656.

[10] Pinker R T. Determination of surface albedo from satellites. Advances in Space Research, 1985; 5(6): 333–343.

[11] Senay G B, Budde M, Verdin J P, Melesse A M. A coupled remote sensing and simplified surface energy balance approach to estimate actual evapotranspiration from irrigated fields. Sensors, 2007; 7(6): 979–1000.

[12] Allen R G, Tasurmi M, Morse A T, Trezza R. A landsat-based energy balance and evapotranspiration model in western US water rights regulation and planning. Journal of Irrigation and Drainage Systems, 2005; 19(3): 251–268.

[13] Idso S B, Jackson R D, Reginato R J. Estimating evaporation: a technique adaptable to remote sensing. Science, 1975; 189(4207): 991–2.

[14] Menenti M. Defining relationships between surface characteristics and actual evaporation rate. Institute for Land and Water Manegement Research, Wageningen, the Netherland, 1979; Monograph No: 109287.

[15] Seguin B, Itier B. Using midday surface temperature to estimate daily evaporation from satellite thermal IR data.

International Journal of Remote Sensing, 1983; 4(2): 371–383.

[16] Kerr Y H, Imbernon J, Dedieu G, Hautecoeur O, Lagouarde J P, Seguin B. NOAA AVHRR and its uses for rainfall and evapotranspiration monitoring. International Journal of Remote Sensing, 1989; 10(4-5): 847–854.

[17] Fischer E, Lawrence D, Sanderson B. Quantifying uncertainties in projections of extremes a perturbed land surface parameter experiment. Climate Dynamics, 2010; 37(7): 1381–1398.

[18] Al-Gaadi K A, Patil V C, Tola E, Madugundu R, Gowda P H. Evaluation of METRIC-derived ET fluxes over irrigated alfalfa crop in desert conditions using scintillometer measurements. Arabian Journal of Geosciences, 2016; 9(6): 441.

[19] Tanner C B, Pelton W L. Potential evapotranspiration estimates by the approximate energy balance method of Penman. Journal of Geophysical Research, 1960; 65(10): 3391–3413.

[20] Blaney H F, Criddle W D. Determining consumptive use for planning water developments. US Department of Agriculture, 1996; No.1275.

[21] Penman H L, Angus D E, Van Bavel C H M. Microclimatic factors affecting evaporation and transpiration. Irrigation of Agricultural Lands, 1967; 483–505.

[22] Christiansen J E. Pan evaporation and evapotranspiration from climatic data. Proceeding of American Society of Civil Engineers, Journal of Irrigation and Drainage, 1968; 18(15): 1725–1732

[23] Jabatan Perangkaan Malaysia. Basic population characteristics by administrative districts. Archived from the original, Kuala Lumpur, 2010; 3.

[24] Perak Town & Districts, Geography & Climate, Economy. Perak Darul Ridzuan, Malaysia. 2012. http://www.malaysia-hotels.net/perak/index.html. Accessed on [2012-10].

[25] Jensen J R. Introductory digital image processing. Third Edition. University of Carolina: Pearson Prentice Hall, 2005.

[26] Hassaballa A A, Matori A B. The estimation of air temperature from NOAA/AVHRR images and the study of NDVI-Ts impact: Case study: The application of split-window algorithms over (Perak Tengah & Manjong) area, Malaysia. International Conference on Space Science and Communication (IconSpace), Malaysia, IEEE. 2011.

[27] Becker F, Li Z L. Temperature-independent spectral indices in thermal infrared bands. Remote Sensing of Environment, 1990; 32(1): 17–33.

[28] Van de Griend A A, Owe M. On the relationship between thermal emissivity and the normalized difference vegetation index for natural surfaces. International Journal of Remote Sensing, 1993; 14: 1119–1131.

[29] Courault D, Seguin B, Olioso A. Review on estimation of evapotranspiration from remote sensing data: From empirical to numerical modeling approaches. Irrigation and Drainage systems, 2005; 19(3): 223–249.

[30] Bastiaanssen W G M. Regionalization of surface flux densities and moisture indicators in composite terrain: a remote sensing approach under clear skies in Mediterranean climates, Land bouwuniversiteit te Wageningen; 1995.

[31] Batra N, Islam S, Venturini V, Bisht G, Jiang L. Estimation and comparison of evapotranspiration from MODIS and AVHRR sensors for clear sky days over the Southern Great Plains. Remote Sensing of Environment. 2006; 103 (1):1–5.

[32] Chemin Y. Evapotranspiration of crops by remote sensing using the energy balance based algorithms. 1ts International Yellow River Forum on River Basin Management, 2003; pp. 76–85.

[33] Nelson B C, Waters R, Kimberly I, Allen R, Tasumi M, Trezza R, et al. Surface energy balance algorithms for land (SEBAL). Advanced Training and User's Manual. The Idaho Department of Water Resources, Idaho. The Idaho Department of Water Resources; 2002.

[34] Sobrino J A, Gomez M, Jiménez-Muñoz J C, Olioso A. Application of a simple algorithm to estimate daily evapotranspiration from NOAA–AVHRR images for the Iberian Peninsula. Remote Sensing of Environment, 2007; 110(2): 139–148.

[35] Bastiaanssen W G M. SEBAL-based sensible and latent heat fluxes in the irrigated Gediz Basin, Turkey. Journal of Hydrology, 2000; 229(1): 87–100

[36] Chatterjee S. Estimating evapotranspiration using remote sensing: A hybrid approach between MODIS derived enhanced vegetation index, Bowen ratio system, and ground based micro-meteorological data. Wright State University, 2010.

[37] Hafeez M M. Water accounting and productivity at different spatial scales in a rice irrigation system. Cuvillier, 2003.

[38] Patil V C, Al-Gaadi K A, Madugundu R, Tola E H, Marey S, Aldosari A, et al. Assessing agricultural water productivity in desert farming system of Saudi Arabia. IEEE Journal of Selected Topics in Applied Earth Observations and Remote Sensing, 2015; 8(1): 284–97.

[39] Shahidian S, Serralheiro R, Serrano P, João Teixeira, José Haie, Naim, et al. Hargreaves and other reduced-set methods for calculating evapotranspiration. Evapotranspiration–Remote Sensing and Modeling, Ayse Irmak Ed. InTech, Croatia, 2012; pp. 59–80.

[40] Hargreaves G H, Samani Z A. Estimating potential evapotranspiration. Journal of the Irrigation and Drainage Division, 1982; (108): 225–230.

[41] Turc L. Evaluation des besoins en eau d'irrigation, évapotranspiration potentielle. Annales Agronomiques, 1961; (12): 13–49.

[42] Pandey P K, Pandey V. Lysimeter based crop coefficients for estimation of crop evapotranspiration of black gram (*Vigna Mungo* L.) in sub-humid region. Int J Agric & Biol Eng, 2012; 4(4): 50–58.